Arch Neurosci. 2024 October; 11(4): e147989 https://doi.org/10.5812/ans-147989

Published Online: 2024 October 22 **Research Article**

# Evaluation the Impressionability of Acellular Scaffolds in Presence of Different Combination of Umbilical Cord Blood Stem Cells and Platelet Rich Fibrin in Repair of Knee Defects in Rabbit (Novel Method with Xeno-Material Elements

Seyed Khalil Pestehei [1], Mahdieh Ghiasi [1,*], Nima Bagheri [2]

[1] Brain and Spinal Cord Injury Research Center, Neuroscience Institute, Tehran University of Medical Sciences, Tehran, Iran
[2] Joint Reconstruction Research Center, Tehran University of Medical Sciences, Tehran, Iran

[*] ***Corresponding Author:*** Brain and Spinal Cord Injury Research Center, Neuroscience Institute, Tehran University of Medical Sciences, Tehran, Iran. Email: mahdieh.ghiasi@yahoo.com

**Received:** 28 April, 2024; **Revised:** 12 August, 2024; **Accepted:** 1 September, 2024

## Abstract

**Background:** Currently, the use of xenogeneic and allogeneic compounds in the treatment of musculoskeletal diseases is common. Repairing bone and cartilage remains a significant challenge for orthopedic surgeons. One of the principal goals of tissue engineering is the development of appropriate scaffolds that can promote tissue regeneration. Various cells and genes are involved in bone and cartilage regeneration, and new scaffolds can induce these processes during osteoregeneration.

**Objectives:** The aim of this study is to evaluate the effects of umbilical cord blood stem cells (USCs) and platelet-rich fibrin (PRF) using acellular scaffolds in the repair of knee defects in rabbits.

**Methods:** In this study, the femoral patella of 12 male New Zealand rabbits was drilled, and they were divided into four groups: (1) control (rabbits with femoral defects), (2) acellular osteochondral (AO), (3) AO + PRF, and (4) AO + USCs / platelet-rich fibrin. Different scaffolds were implanted into their knees, and after six months, histological evaluations were conducted. To further investigate the effects of scaffolds on bone and cartilage, gene expression levels of Col 1, Col X, Runx2, SOX9, and ALP were measured using real-time PCR.

**Results:** All the implanted materials contributed to knee repair. In terms of statistical analysis, the use of USCs and platelet-rich fibrin with natural scaffolds such as Acellular Osteochondral provided better results for repairing bone and cartilage. The evaluation of specific bone regeneration genes (COLI, RUNX2) and the histological results from the implanted site in experimental osteochondral defects indicated that the most effective knee repair occurred in the group treated with cell-free osteochondral scaffolds, USCs, and platelet-rich fibrin.

**Conclusions:** This study demonstrates that the combination of biomaterials and xenografts can accelerate the regeneration process.

*Keywords:* Acellular Scaffolds, Bone and Cartilage Defects, Platelet Rich Fibrin, Umbilical Cord Blood Stem Cells

## 1. Background

Repairing massive bone and cartilage loss remains a significant challenge for orthopedic surgeons. The regeneration of both cartilage and bone has proven to be difficult due to their distinct physiological structures and functions (1). Most defects are typically caused by factors such as physiological bone resorption secondary to tooth loss, trauma, bone pathologies, or infections, leading to osteochondral (OC) defects (2). Osteochondral defects affect the superficial cartilage region, intermediate calcified cartilage, and subchondral bone, severely impacting patients' health and quality of life (3). One of the key objectives of Bone Tissue Engineering (BTE) is to design biodegradable scaffolds with appropriate porosity that integrate natural elements and molecular cues to foster tissue regeneration (4). Umbilical stem cells (USCs) have shown potential in promoting regeneration. Recent advancements in strategies for isolating, expanding,

and shortening the timing of USC engraftment have significantly enhanced transplantation efficacy (5).

Bone formation consists of a series of complex events during the differentiation of mesenchymal stem cells into osteoblasts. Bone morphogenetic proteins (BMPs) play a crucial role in osteoblast differentiation by promoting the production of bone-specific matrix proteins (6). BMP-2, a key growth factor in the BMP subfamily, regulates osteoblast differentiation by stimulating osteoblast-related transcription factors, including runt-related transcription factor 2 (Runx2), alkaline phosphatase (ALP), Collagen I (Col 1) (7), Collagen 10 (Col X) (8), and SOX9 (9, 10).

In the last two decades, several therapeutic approaches have been explored for bone regeneration, including scaffold-free and cell-based methods, as well as advanced treatments combining cells with various biomaterials (11). Biological scaffolds, derived from decellularized tissues and organs, have garnered significant attention because they can provide mechanical and chemical signals that promote cell attachment and differentiation in tissue regeneration (12). These scaffolds are influenced by both physical and procedural decellularization factors (13). Non-synthetic polymers, such as collagen, chitosan, starch, hyaluronic acid, and alginate, tend to have weaker and softer structures compared to ceramics but are recommended due to their flexibility and ability to conform to various shapes (14). Moreover, naturally sourced polymers can protect and guide cells during multiple stages of their proliferation, thanks to the presence of specific molecular domains, leading to biological interaction between the scaffold and the host tissue (7, 15).

Platelet-rich fibrin (PRF) is considered a platelet product and fibrin network that contains growth factors, cytokines, and cells. These factors are gradually released over time, making PRF useful as a biological membrane in various surgical applications (8). Osteochondral tissue engineering has shown significant progress in developing techniques for regenerating damaged cartilage and bone tissues.

Due to the limited self-repair capacity of cartilage tissue, it is essential to develop biomaterial-based approaches with different structures. Given the role of key genes in osteoregeneration and the growing need for more cost-effective, rapid, and novel bone regeneration methods, this study evaluated the histological impact of acellular scaffolds in combination with stem cells derived from cord blood and platelet-rich fibrin.

## 2. Objectives

Additionally, the expression of Col 1, Col X, Runx2, SOX9, and ALP genes was investigated in the repair of knee defects in rabbits.

## 3. Methods

### 3.1. Prepration of Acellular Scaffolds

Osteochondral samples were obtained from the femoral patella of ovine bone marrow and transferred to the laboratory for freeze-thaw processing. Initially, the fragments were washed twice with phosphate-buffered saline. The samples then underwent four freeze-thaw cycles, where they were frozen at -121 degrees Celsius for 20 minutes and subsequently placed in liquid nitrogen. After each cycle, the blocks were washed with distilled water. To remove cellular debris, the blocks were treated with 1% Triton X-100 for 8 hours, followed by an additional treatment for 16 hours. To eliminate any remaining detergent, the samples were washed twice with distilled water for 24 rounds. The entire procedure was carried out using a rotator at room temperature.

### 3.2. Platelet-Rich Fibrin Preparation

Platelet-rich fibrin was prepared by drawing 20 mL of blood from a single candidate and transferring it into 10 mL sterile tubes without any anticoagulant. All samples were centrifuged at 2700 rpm for 3 minutes. The upper layer of each tube was collected and stored in sterile syringes for scaffold fabrication. Subsequently, the PRF structure was lyophilized and stored in a -20°C freezer until use.

### 3.3. Cell Culture

After receiving USCs from healthy donors, they were transferred to the laboratory for stem cell isolation processing. Initially, the umbilical cord was washed three times with phosphate buffer saline, then fragmented and digested with type I collagenase for 30 minutes at 37°C. The cells were treated with DMEM-low glucose (1 g/liter) and incubated at 37°C. After 24 hours, the adherent cells were cultured and prepared for the study.

### 3.4. Loading the Different Combination of Stem Cells Derived Cord Blood and Platelet Rich Fibrin on Acellular Scaffolds

The scaffolds were wetted in DMEM medium and incubated for 1 hour. After removing the medium, $1 \times 10^6$ stem cells derived from cord blood and platelet-rich

fibrin were loaded onto the scaffolds and incubated for an additional 2 hours.

### 3.5. Preparation of Animal and Histology

In this study, 12 male New Zealand rabbits, with a mean weight of 1.300 - 1.500 kg, were housed in the animal facility at Tehran Medical University, following approval from the Ethics Committee (Approval ID: IR.TUMS.AEC.1402.070). A hole measuring 4.5 mm in diameter and 4 mm in depth was drilled in the femoral patella of each rabbit's knee. The rabbits were divided into four groups (3 rabbits per group): (1) control (OC), (2) acellular osteochondral (AO), (3) acellular osteochondral + PRF, and (4) acellular osteochondral + stem cells derived from cord blood/platelet rich fibrin. The defect in the femoral patella was treated with scaffolds in groups 2, 3, and 4. Six months post-operation, the implanted tissues were harvested and transferred to 10% neutral buffered formalin (NBF, pH 7.26) for 48 hours. The samples were then decalcified in 10% formic acid for 10 days and processed. Sections of 5µm thickness were stained with Hematoxylin and Eosin (H&E), Masson's Trichrome (MT), and Safranin O (SO).

### 3.6. Analysis of Real time Polymerase Chain Reaction (PCR)

Using Trizol (Invitrogen, USA), total RNA was extracted. The RNA purity was assessed by measuring the absorbance at 260 nm and 280 nm (Nanodrop, Biotek, USA). The extracted RNA was then reverse transcribed into complementary DNA (cDNA) using a Takara kit (Japan). The expression levels of mRNA transcripts were quantified through real-time PCR (Rotor Gene 6000, Corbett, Australia). The PCR product detection was based on the fluorescence enhancement observed from the binding of SYBR Green to double-stranded DNA. Specific primers were used for the following genes: SOX9 (forward: 5'-GGCAGCTGTGAACTGGCCA-3', reverse: 5'-GCACACGGGGAACTTGTCC-3') (18), collagen type I (forward: 5'–CGGCTCCTGCTCCTCTTAGCG–3', reverse: 5'–CTGTACGCAGGTGACTGGTG–3') (18), Runx2 (forward: 5'–GACTGTGGTTACCGTCATGGC–3', reverse: 5'–ACTTGGTTTTTCATAACAGCGGA–3'), Col X (forward: 5'–GAAAACCAGGCTATGGAACC–3', reverse: 5'–GCTCCTGTAAGTCCCTGTTGTC–3'), and ALP (forward: 5'–TGTGCGGGGTCAAGGCTAAC–3', reverse: 5'–GGCGTCCGAGTACCAGTTGC–3') (19), which were designed using Primer3 software. The following PCR conditions were applied: 94°C for 15 min, followed by 45 cycles at 94°C for 15 s, 58°C for 30 s, and 72°C for 30 s. GAPDH (forward: 5'–CTGGTGCTGAGTACGTGGTG–3', reverse: 5'–CGTCAGCAGAAGGTGCAGAG–3') was used as a housekeeping gene to normalize the RNA quantity and quality.

### 3.7. Statistical Analysis

The analysis of variance (ANOVA) was utilized to assess the significance of new bone and blood vessel formation, using GraphPad Prism software, Version 6.00 (GraphPad Prism, Inc., San Diego, CA). A significance level was set at $P < 0.05$.

## 4. Results

### 4.1. Acellular Scaffolds and Isolation of Stem Cells Derived Cord Blood and Platelet Rich Fibrin

The cells from the sample fragments were removed, and the scaffolds were prepared for implantation. The decellularized scaffold was confirmed histologically (Figure 1). Stem cells derived from cord blood and plasma rich fibrin were isolated from the blood, and the scaffolds were exposed to these components for implantation (Figure 2).

### 4.2. Histopathological and Radiological Analysis

The scaffolds were implanted into the femoral patella of rabbits in groups 2, 3, and 4. As illustrated in Figure 3, the various stages of implantation include: A and B show the acellular scaffold, C and D depict the skin incision, E shows the muscle incision, and F illustrates the implantation of the scaffold. Histological sections were examined 6 months post-implantation. In the control group (untreated), the defect site was completely repaired with fibrous connective tissue (FCT), and an accumulation of inflammatory cells (ICs) was evident. In the group treated with the acellular osteochondral graft, the defect area was replaced with a combination of neo-bone and fibrocartilage. Additionally, tendon-like tissue (connective tissue) had accidentally entered the defect site. The immaturity of fibrocartilage tissue was confirmed using the Safranin O (SO) staining technique. The stained images of the osteochondral area in the AO+PRF-treated group showed the formation of new bone and cartilage, with a significantly higher amount of cartilaginous tissue compared to normal tissue. Furthermore, mineralization of the fibrocartilage tissue was observed on a large scale. In the AO + PRF + cell group, new bone maturation was considerably higher than in other groups. The implanted material was fully recellularized, and most of the desired tissue was hyaline cartilage, with the cartilage layer showing normal thickness (Figure 4).

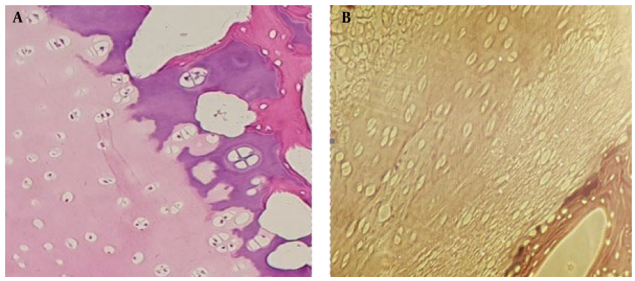


**Figure 1.** Osteochondral fragments. A, the cellular; and B, acellular

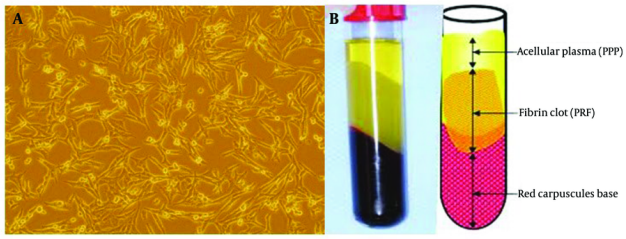


**Figure 2.** A, stem cells derived cord blood; and B, platelet Rich Fibrin

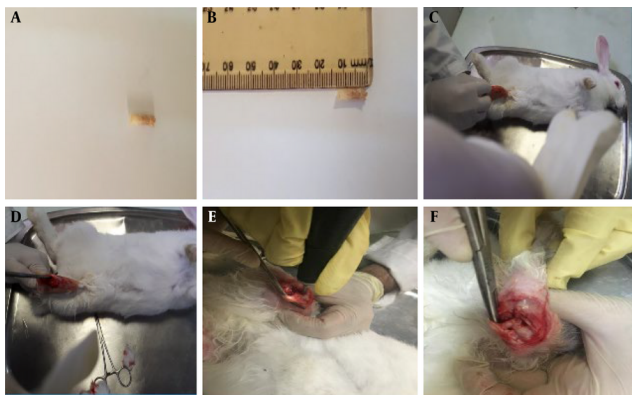


**Figure 3.** A and B, acellular scaffold; C and D, cutting the skin; E, cutting the muscle; F, implantation of scaffold.

Overall, no foreign body reactions or severe inflammatory responses were observed. The AO+PRF-cell and AO+PRF groups exhibited significant new bone ingrowth (65 ± 6%), whereas the free AO group did not show significant new bone formation (4 ± 1%). Hyaline cartilage was formed in the AO+PRF-cell treated group. The amount of new tissue was significantly higher in the AO+PRF (158 ± 13) and AO + PRF + cell (1 ± 11) groups compared to the AO (62 ± 8) and control groups, as determined by histomorphometric analysis (Table 1).

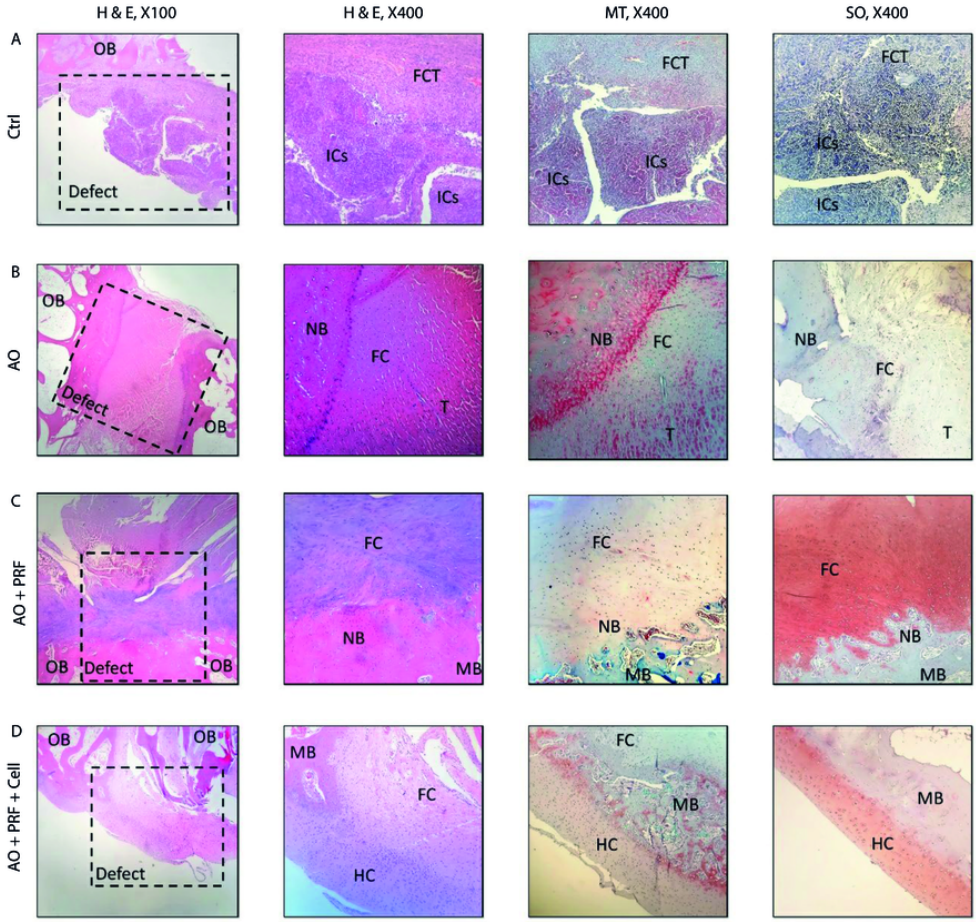


**Figure 4.** The findings of Histopathological in defect of osteochondral in the experimental groups. A, in the control group (untreated), the area of osteochondral defect was completely replaced with fibrous connective tissue (FCT) and the accumulation of inflammatory cells (ICs) was evident; B, in Acellular Osteochondral graft, the implanted graft completely filled by two types of tissue: Neo-bone and immature fibrocartilage (SO staining); C, the osteochondral defect in OA + PRF treated group showed new bone and cartilage formation, however, the amount of cartilaginous tissue was significantly higher than normal tissue; D, the maturation of new bone in OA + PRF + cell treated animals was significantly higher than other treatment groups. In addition, the thickness of the cartilage layer was normal. OB: Old Bone, NB: New Bone formation, ICs: Inflammatory Cells. FC: Fibrocartilage, HC: Hyaline cartilage, FCT: Fibrous Connective Tissue, T: Tendon-like tissue, MB: Mature bone.

This demonstrated good biocompatibility in all experimental groups (Table 2).

### *4.3. Chondrogenic Gene Expression Assessment by Real time PCR*

The results of Col 1 gene expression showed a significant decrease in the AO + PRF group (P = 0.003) compared to the Control group (0.25 or 2.86-fold). The other groups showed an increase: AO group by 1.11-fold and AO + PRF + Cell group by 1.52-fold; however, these increases were not statistically significant, with p = 0.649 and P = 0.137, respectively, compared to the Control group.

The expression level of Col X gene in the AO group demonstrated a significant decrease (P = 0.005) compared to the other three groups. Although the level of Col X increased in the AO + PRF group, the change was not statistically significant (P = 0.325). The effect of AO and AO + PRF + Cell on the mRNA expression of SOX9 was significant with P = 0.012 and p = 0.036, respectively.

The ALP gene expression showed a significant increase in both the AO group (P = 0.039) and the AO + PRF group (P = 0.024) compared to the Control group.

Additionally, the Runx2 gene expression showed significant changes across all groups compared to the Control group. The AO group had a 7.31-fold increase (P =

**Table 1.** Histomorphometric Findings of Regenerated Tissue in the Defect Area [a, b]

| Valuable | Ctrl | AO | AO + PRF | AO + PRF + Cell |
|---|---|---|---|---|
| **Fibroblast + fibrocyte** | 202.0 ± 28.0 | 32.0 ± 10.4 [c] | 13.7 ± 5.1 [d] | 4.5 ± 1.07 [d] |
| **Osteoblast + osteocyte** | 3.5 ± 3.4 | 18.5 ± 3.4 [e] | 199.7 ± 26.4 [d] | 100.0 ± 12.9 [c] |
| **Chondroblast + chondrocyte** | 0 | 125.7 ± 5.7 [c] | 146.7 ± 7.8 [c] | 233.2 ± 16.5 [d] |

[a] Values indicates treatment group versus negative control group (C-).

[b] Values are expressed as mean ± SD.

[c] $P < 0.01$.

[d] $P < 0.001$.

[e] $P < 0.05$.

**Table 2.** The New Cartilage (%) and new Bone Formation (%) in Osteochondral Defect [a, b]

| Groups | New Cartilage Tissue (%) | New Bone Formation (%) |
|---|---|---|
| **Ctrl** | 0 [A] | 1.6 ± 1.1 [A] |
| **AO** | 10.3 ± 2.5 [B] | 18 ± 2 [B] |
| **AO + PRF** | 43 ± 4.3 [C] | 45.3 ± 5.1 [C] |
| **AO + PRF + Cell** | 48 ± 5 [C] | 32 ± 3.6 [C] |

[a] Different letters indicate significant differences between the treatment group.

[b] Values are expressed as mean ± SD.

0.000), the AO + PRF group had a 2.32-fold increase ($P = 0.031$), and the AO + PRF + Cell group had an 11.2-fold increase ($P = 0.000$) (Figure 5).

## 5. Discussion

Our results have shown that the simultaneous use of scaffolds, such as acellular osteochondral, with stem cells like stem cell-derived cord blood and PRF, can effectively accelerate the regeneration process for OC defects in animal models. As observed in the histological analysis, the maturation of new bone and cartilage in the OA + PRF + Cell group was significantly higher compared to the other groups. Additionally, our radiological results indicated that the healed bone exhibited less density when PRF was used as the sole filling material, especially when combined with stem cells. This outcome is expected, as PRF is considered a membrane with soft tissue density (16). In a similar study conducted by Zhang et al. in 2017, it was demonstrated that platelet concentrations in PRP samples were 4.9 times higher than in whole blood samples, and the histological analysis of neo-tissue in samples treated with scaffolds and autologous PRP showed subchondral bone formation in a rabbit model (17).

Recently, natural scaffolds have garnered increased attention due to their ability to provide mechanical and chemical signals for cell attachment and differentiation in tissue regeneration. Scaffolds such as platelet-rich plasma (PRP) and PRF are new biological tools in tissue engineering and are widely used by surgeons and dentists. Moreover, various studies have shown positive outcomes with the application of PRF, either as a sole filler or in different combinations, delivering satisfactory results (18, 19).

In this study, we evaluated the expression of five genes involved in articular cartilage degeneration, osteoarthritis, repair, regeneration, and transplantation. Col I is an osteogenesis-related gene and serves as an ideal marker for bone regeneration (20-22). In this study, the expression of the Col I gene showed a significant decrease in the AO + PRF group, indicating a reduction in tissue degeneration within this group.

SOX9 is a key cartilage matrix protein that regulates and expresses itself alongside type II collagen (Col II) and Col I (23). Researchers have demonstrated that collagen type I and X (COL I, COL X) genes express

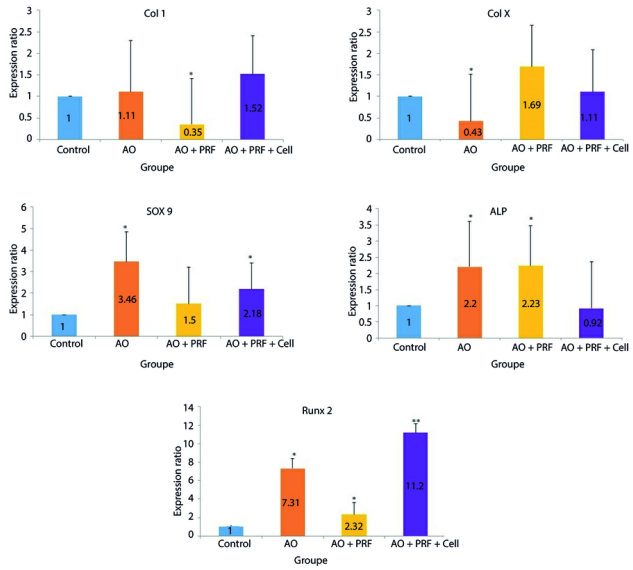


**Figure 5.** The graphs show the expression of Col 1, Col X, SOX9, ALP and Runx 2 in 3 groups (AO (acellular osteochondral), AO + PRF (acellular osteochondral + platelet rich fibrin) and AO + PRF + cell (acellular osteochondral +stem cells derived cord blood/ platelet rich fibrin)) compared with the control group. Overall, the expression of Col 1 in AO + PRF group, Col X in AO group, SOX9 in AO and AO + PRF + Cell group, ALP in AO and AO + PRF group and Runx2 in all group have shown significant difference compared with Control group. Data are determined as means ± SD; *P < 0.05; **P < 0.01.

hypertrophy-related proteins (24). The Col X content was lower in the AO group, which correlated with enhanced bone generation (25).

In terms of ALP gene expression, the AO + PRF + Cell group showed a decrease compared to the AO and AO + PRF groups. ALP is considered an early marker of osteoblast differentiation and tends to increase in osteochondral defects (26). However, the simultaneous implantation of acellular osteochondral scaffolds, stem cells, and plasma-rich fibrin was shown to reduce this expression in the animal model.

On the other hand, Runx2 gene expression significantly increased in all three groups. During the development of osteochondral defects, the hypertrophic process occurs alongside the differentiation of articular chondrocytes. Runx2 plays a fundamental role in regulating key genes involved in chondrocyte/osteoblast differentiation and matrix degradation (27, 28). Many studies have demonstrated that Runx2 expression levels are elevated in human osteochondral defects. To investigate the role of Runx2 in the development of osteochondral defects, genetic animal models have been utilized. Overexpression of Runx2 in mice has been shown to increase the expression of cartilage proteases in chondrocyte cells (29, 30). This also leads to the activation of matrix degradation enzymes, such as MMP13 and ADAMTS5, through the mitogen-activated protein kinase (MAPK) pathways (31), and directly regulates MMP13 gene transcription (32). It is now understood that the implantation of scaffolds, along with a large number of cells, is necessary for the repair of osteochondral defects. However, Hansen et al. reported that increasing cell seeding density did not have a positive effect on cartilage repair (33). The results of this study indicate that selecting the best materials is crucial for the reconstruction process, which requires further research in the field of tissue engineering.

### 5.1. Conclusions

In conclusion, the use of stem cells and plasma-rich fibrin in combination with natural scaffolds, such as acellular osteochondral scaffolds, can serve as an effective filler for repairing bone and cartilage in medical applications. However, evaluating more genes and proteins in other animals and different parts of the skeletal system could provide a deeper understanding of these biomaterials.

## Acknowledgements

I would like to express my special thanks of gratitude to my teacher M.A who help me in doing surgery.

## Footnotes

**Authors' Contribution:** Study concept and design: M. Gh.; analysis and interpretation of data: M. Gh., and Kh. P.; drafting of the manuscript: M. Gh.; critical revision of the manuscript for important intellectual content: M. Gh., N. B., and Kh. P.; statistical analysis: M. Gh.

**Conflict of Interests Statement:** The authors declared no conflict of interests.

**Data Availability:** The dataset presented in the study is available on request from the corresponding author during submission or after its publication. The data are not publicly available due to restriction by other authors.

**Ethical Approval:** IR.TUMS.AEC.1402.070 .

**Funding/Support:** This study was supported in part by grant 1402-2-146-65536 from Brain and Spinal Cord Injury Research Center, Neuroscience Institute, Tehran University of Medical Sciences, Tehran, Iran.

## References

1. Vidal L, Kampleitner C, Brennan MA, Hoornaert A, Layrolle P. Reconstruction of Large Skeletal Defects: Current Clinical Therapeutic Strategies and Future Directions Using 3D Printing. *Front Bioeng Biotechnol*. 2020;**8**:61. [PubMed ID: 32117940]. [PubMed Central ID: PMC7029716]. https://doi.org/10.3389/fbioe.2020.00061.
2. Wang Y, Zhang W, Yao Q. Copper-based biomaterials for bone and cartilage tissue engineering. *J Orthop Translat*. 2021;**29**:60-71. [PubMed ID: 34094859]. [PubMed Central ID: PMC8164005]. https://doi.org/10.1016/j.jot.2021.03.003.
3. Cai H, Yao Y, Xu Y, Wang Q, Zou W, Liang J, et al. A Col I and BCP ceramic bi-layer scaffold implant promotes regeneration in osteochondral defects. *RSC Adv*. 2019;**9**(7):3740-8. [PubMed ID: 35518063]. [PubMed Central ID: PMC9060255]. https://doi.org/10.1039/c8ra09171d.
4. Selaru A, Herman H, Vlasceanu GM, Dinescu S, Gharbia S, Balta C, et al. Graphene-Oxide Porous Biopolymer Hybrids Enhance In Vitro Osteogenic Differentiation and Promote Ectopic Osteogenesis In Vivo. *Int J Mol Sci*. 2022;**23**(1). [PubMed ID: 35008918]. [PubMed Central ID: PMC8745160]. https://doi.org/10.3390/ijms23010491.
5. Shang Y, Guan H, Zhou F. Biological Characteristics of Umbilical Cord Mesenchymal Stem Cells and Its Therapeutic Potential for Hematological Disorders. *Front Cell Dev Biol*. 2021;**9**:570179. [PubMed ID: 34012958]. [PubMed Central ID: PMC8126649]. https://doi.org/10.3389/fcell.2021.570179.
6. Huntley R, Jensen E, Gopalakrishnan R, Mansky KC. Bone morphogenetic proteins: Their role in regulating osteoclast differentiation. *Bone Rep*. 2019;**10**:100207. [PubMed ID: 31193008]. [PubMed Central ID: PMC6513777]. https://doi.org/10.1016/j.bonr.2019.100207.
7. Deng C, Chang J, Wu C. Bioactive scaffolds for osteochondral regeneration. *J Orthop Translat*. 2019;**17**:15-25. [PubMed ID: 31194079]. [PubMed Central ID: PMC6551354]. https://doi.org/10.1016/j.jot.2018.11.006.
8. Talebi Ardakani MR, Meimandi M, Shaker R, Golmohammadi S. The Effect of Platelet-Rich Fibrin (PRF), Plasma Rich in Growth Factors (PRGF), and Enamel Matrix Proteins (Emdogain) on Migration of Human Gingival Fibroblasts. *J Dent (Shiraz)*. 2019;**20**(4):232-9. [PubMed ID: 31875169]. [PubMed Central ID: PMC6890812]. https://doi.org/10.30476/DENTJODS.2019.44917.
9. Phimphilai M, Zhao Z, Boules H, Roca H, Franceschi RT. BMP signaling is required for RUNX2-dependent induction of the osteoblast phenotype. *J Bone Miner Res*. 2006;**21**(4):637-46. [PubMed ID: 16598384]. [PubMed Central ID: PMC2435171]. https://doi.org/10.1359/jbmr.060109.
10. Yan YL, Willoughby J, Liu D, Crump JG, Wilson C, Miller CT, et al. A pair of Sox: distinct and overlapping functions of zebrafish sox9 co-orthologs in craniofacial and pectoral fin development. *Development*. 2005;**132**(5):1069-83. [PubMed ID: 15689370]. https://doi.org/10.1242/dev.01674.
11. Maia FR, Carvalho MR, Oliveira JM, Reis RL. Tissue Engineering Strategies for Osteochondral Repair. *Adv Exp Med Biol*. 2018;**1059**:353-71. [PubMed ID: 29736582]. https://doi.org/10.1007/978-3-319-76735-2_16.
12. Starnecker F, Konig F, Hagl C, Thierfelder N. Tissue-engineering acellular scaffolds-The significant influence of physical and procedural decellularization factors. *J Biomed Mater Res B Appl Biomater*. 2018;**106**(1):153-62. [PubMed ID: 27898187]. https://doi.org/10.1002/jbm.b.33816.
13. Zhang X, Chen X, Hong H, Hu R, Liu J, Liu C. Decellularized extracellular matrix scaffolds: Recent trends and emerging strategies in tissue engineering. *Bioactive materials*. 2022;**10**:15-31. https://doi.org/10.1016/j.bioactmat.2021.09.014.
14. Ghiasi M, Mehdizadeh M, Sharifi AM, Tafvizi F, Safari S, Maroof NT. Use of mesenchymal adult stem cell for cartilage regeneration by hydrogel. *International Journal of Medical Laboratory*. 2019. https://doi.org/10.18502/ijml.v6i3.1403.
15. Sheykhhasan M, Qomi RT, Kalhor N, Mehdizadeh M, Ghiasi M. Evaluation of the ability of natural and synthetic scaffolds in providing an appropriate environment for growth and chondrogenic differentiation of adipose-derived mesenchymal stem cells. *Indian J Orthop*. 2015;**49**(5):561-8. [PubMed ID: 26538764]. [PubMed Central ID: PMC4598549]. https://doi.org/10.4103/0019-5413.164043.
16. Serafini G, Lopreiato M, Lollobrigida M, Lamazza L, Mazzucchi G, Fortunato L, et al. Platelet Rich Fibrin (PRF) and Its Related Products: Biomolecular Characterization of the Liquid Fibrinogen. *J Clin Med*. 2020;**9**(4). [PubMed ID: 32290550]. [PubMed Central ID: PMC7230328]. https://doi.org/10.3390/jcm9041099.
17. Zhang YT, Niu J, Wang Z, Liu S, Wu J, Yu B. Repair of Osteochondral Defects in a Rabbit Model Using Bilayer Poly(Lactide-co-Glycolide) Scaffolds Loaded with Autologous Platelet-Rich Plasma. *Med Sci Monit*. 2017;**23**:5189-201. [PubMed ID: 29088126]. [PubMed Central ID: PMC5676501]. https://doi.org/10.12659/msm.904082.
18. Del Corso M, Vervelle A, Simonpieri A, Jimbo R, Inchingolo F, Sammartino G, et al. Current knowledge and perspectives for the use of platelet-rich plasma (PRP) and platelet-rich fibrin (PRF) in oral and maxillofacial surgery part 1: Periodontal and dentoalveolar surgery. *Curr Pharm Biotechnol*. 2012;**13**(7):1207-30. [PubMed ID: 21740371]. https://doi.org/10.2174/138920112800624391.
19. Shivashankar VY, Johns DA, Vidyanath S, Sam G. Combination of platelet rich fibrin, hydroxyapatite and PRF membrane in the management of large inflammatory periapical lesion. *J Conserv Dent*.

2013;**16**(3):261-4. [PubMed ID: 23833463]. [PubMed Central ID: PMC3698593]. https://doi.org/10.4103/0972-0707.111329.

20. Li Y, Liu Y, Li R, Bai H, Zhu Z, Zhu L, et al. Collagen-based biomaterials for bone tissue engineering. *Materials & Design*. 2021;**210**:110049. https://doi.org/10.1016/j.matdes.2021.110049.
21. Nguyen TT, Jang YS, Kim YK, Kim SY, Lee MH, Bae TS. Osteogenesis-Related Gene Expression and Guided Bone Regeneration of a Strontium-Doped Calcium-Phosphate-Coated Titanium Mesh. *ACS Biomater Sci Eng*. 2019;**5**(12):6715-24. [PubMed ID: 33423489]. https://doi.org/10.1021/acsbiomaterials.9b01042.
22. Yi SW, Kim HJ, Oh HJ, Shin H, Lee JS, Park JS, et al. Gene expression profiling of chondrogenic differentiation by dexamethasone-conjugated polyethyleneimine with SOX trio genes in stem cells. *Stem Cell Res Ther*. 2018;**9**(1):341. [PubMed ID: 30526665]. [PubMed Central ID: PMC6286596]. https://doi.org/10.1186/s13287-018-0998-7.
23. Sutherland AJ, Beck EC, Dennis SC, Converse GL, Hopkins RA, Berkland CJ, et al. Decellularized cartilage may be a chondroinductive material for osteochondral tissue engineering. *PLoS One*. 2015;**10**(5). e0121966. [PubMed ID: 25965981]. [PubMed Central ID: PMC4428768]. https://doi.org/10.1371/journal.pone.0121966.
24. He A, Liu L, Luo X, Liu Y, Liu Y, Liu F, et al. Repair of osteochondral defects with in vitro engineered cartilage based on autologous bone marrow stromal cells in a swine model. *Sci Rep*. 2017;**7**:40489. [PubMed ID: 28084417]. [PubMed Central ID: PMC5234019]. https://doi.org/10.1038/srep40489.
25. Lin TH, Wang HC, Cheng WH, Hsu HC, Yeh ML. Osteochondral Tissue Regeneration Using a Tyramine-Modified Bilayered PLGA Scaffold Combined with Articular Chondrocytes in a Porcine Model. *Int J Mol Sci*. 2019;**20**(2). [PubMed ID: 30650528]. [PubMed Central ID: PMC6359257]. https://doi.org/10.3390/ijms20020326.
26. Shen C, Yang C, Xu S, Zhao H. Comparison of osteogenic differentiation capacity in mesenchymal stem cells derived from human amniotic membrane (AM), umbilical cord (UC), chorionic membrane (CM), and decidua (DC). *Cell Biosci*. 2019;**9**:17. [PubMed ID: 30792848]. [PubMed Central ID: PMC6371545]. https://doi.org/10.1186/s13578-019-0281-3.
27. Chen D, Kim DJ, Shen J, Zou Z, O'Keefe RJ. Runx2 plays a central role in Osteoarthritis development. *J Orthop Translat*. 2020;**23**:132-9. [PubMed ID: 32913706]. [PubMed Central ID: PMC7452174]. https://doi.org/10.1016/j.jot.2019.11.008.
28. Chen CG, Thuillier D, Chin EN, Alliston T. Chondrocyte-intrinsic Smad3 represses Runx2-inducible matrix metalloproteinase 13 expression to maintain articular cartilage and prevent osteoarthritis. *Arthritis Rheum*. 2012;**64**(10):3278-89. [PubMed ID: 22674505]. [PubMed Central ID: PMC3544176]. https://doi.org/10.1002/art.34566.
29. Hasegawa A, Nakahara H, Kinoshita M, Asahara H, Koziol J, Lotz MK. Cellular and extracellular matrix changes in anterior cruciate ligaments during human knee aging and osteoarthritis. *Arthritis Res Ther*. 2013;**15**(1):R29. [PubMed ID: 23406989]. [PubMed Central ID: PMC3672799]. https://doi.org/10.1186/ar4165.
30. Kadri A, Funck-Brentano T, Lin H, Ea HK, Hannouche D, Marty C, et al. Inhibition of bone resorption blunts osteoarthritis in mice with high bone remodelling. *Ann Rheum Dis*. 2010;**69**(8):1533-8. [PubMed ID: 20525838]. https://doi.org/10.1136/ard.2009.124586.
31. Tetsunaga T, Nishida K, Furumatsu T, Naruse K, Hirohata S, Yoshida A, et al. Regulation of mechanical stress-induced MMP-13 and ADAMTS-5 expression by RUNX-2 transcriptional factor in SW1353 chondrocyte-like cells. *Osteoarthritis Cartilage*. 2011;**19**(2):222-32. [PubMed ID: 21094261]. https://doi.org/10.1016/j.joca.2010.11.004.
32. Wang M, Tang D, Shu B, Wang B, Jin H, Hao S, et al. Conditional activation of beta-catenin signaling in mice leads to severe defects in intervertebral disc tissue. *Arthritis Rheum*. 2012;**64**(8):2611-23. [PubMed ID: 22422036]. [PubMed Central ID: PMC3632450]. https://doi.org/10.1002/art.34469.
33. Hansen OM, Foldager CB, Christensen BB, Everland H, Lind M. Increased chondrocyte seeding density has no positive effect on cartilage repair in an MPEG-PLGA scaffold. *Knee Surg Sports Traumatol Arthrosc*. 2013;**21**(2):485-93. [PubMed ID: 22488013]. https://doi.org/10.1007/s00167-012-1996-4.